Available online at www.sciencedirect.com
ScienceDirect
Journal of Sound and Vibration 322 (2009) 690–706
JOURNAL OF SOUND AND VIBRATION
www.elsevier.com/locate/jsvi

Grey forecasting model for active vibration control systems

Zou Lihua[a,*], Dai Suliang[a], John Butterworth[b], Xing Ma[b], Bo Dong[a], Aiping Liu[a]

[a]*Department of Civil Engineering, Lanzhou Jiaotong University, Lanzhou 730070, PR China*
[b]*Department of Civil and Environmental Engineering, University of Auckland, Auckland 1142, New Zealand*

Received 2 June 2007; received in revised form 11 November 2008; accepted 15 November 2008
Handling Editor: L.G. Tham
Available online 5 February 2009

Abstract

Based on the grey theory, a GM(1,1) forecasting model and an optimal GM(1,1) forecasting model are developed and assessed for use in active vibration control systems for earthquake response mitigation. After deriving equations for forecasting the control state vector, design procedures for an optimal active control method are proposed. Features of the resulting vibration control and the influence on it of time-delay based on different sampling intervals of seismic ground motion are analysed. The numerical results show that the forecasting models based on the grey theory are reliable and practical in structural vibration control fields. Compared with the grey forecasting model, the optimal forecasting model is more efficient in reducing the influences of time-delay and disturbance errors.

0. Introduction

Vibration control technologies including passive, active, semi-active, and hybrid control of engineering structures have been investigated theoretically and experimentally for more than 30 years. Different control systems have been applied in buildings, bridges, and other structures [1,2,3]. Amongst the competing systems, the active control method has attracted increasing attention of late due to its excellent performance and wide applicability. However, a number of problems have arisen when developing large scale practical applications. One of these relates to the consequences of time-delay within the control system. The control process involves measuring response data, computing control forces and transmitting control signals (CSs) to the actuators. Application of unsynchronized control forces due to time-delay (latency) in the control system will inevitably result in degradation of the control performance. A small time-delay may do no more than reduce the potential benefits of the control process, whereas a large time-delay may cause failure of the control process leading to possible magnification of the structural response and potential instability or failure of the host structure [4,5].

Two common methods for solving the time-delay problem are the time-delay compensation method and the forecasting control method. A number of time-delay compensation methods [6,7] have been studied numerically and experimentally, but some limitations remain. For example, the controller is often derived on the basis of modified state feedback without simultaneous consideration of the time-delay effect, with the

*Corresponding author. Tel.: +86 0931 4939213; fax: +86 0931 4938137.
E-mail address: Zoulihua66@163.com (Z. Lihua).

0022-460X/$ - see front matter © 2009 Elsevier Ltd. All rights reserved.
doi:10.1016/j.jsv.2008.11.036

result that system stability cannot be guaranteed, especially when the time-delay becomes large. The forecasting control method is one of the more effective methods for mitigating the effects of time-delay. There are many forecasting theories, one of which is neural network forecasting. It is suitable for civil engineering control, but needs a large quantity of input data and multi-step training to enable the neural network to gain adequate forecasting precision. The associated numerical computation is intensive. In comparison, grey theory forecasting models [8,9] are not dependent on accurate structural models and need only a few samples. The structure is controlled by active synchronization control forces obtained by predicting the state vector of the structure for the next step. It is possible by this means to exert satisfactory control over the behaviour of the target structure.

One purpose of this paper is to investigate vibration control of structures based on the grey theory forecasting model GM(1,1). To improve the forecast precision, an optimal grey forecasting GM(1,1) model is proposed on the basis of the optimization of the background value. In the optimal grey model, after the state vectors have been forecast, the immediate active optimal control is applied, based on the modern control theories (LQR). Numerical results show that a higher forecasting precision is achieved by using the optimal forecasting GM(1,1) model. The corresponding design procedures are also shown to be functional and effective.

1. Equations of motion of structural systems

1.1. Base-isolation hybrid control system

The building model and corresponding analytical model of a base-isolation hybrid control system [10] are shown in Figs. 1 and 2, respectively. The equation of motion of the structural system is given by

$$[M]\{\ddot{Y}(t)\} + [C]\{\dot{Y}(t)\} + [K]\{Y(t)\} = D_s F(t) + B_s U(t) \tag{1}$$

where $[M]$, $[C]$, and $[K]$ represent the $(n+1)\times(n+1)$ mass, damping, and stiffness matrices of the system, respectively; $Y(t)$, $\dot{Y}(t)$, and $\ddot{Y}(t)$ represent the $(n+1)$-dimensional vectors of structural inter-storey displacement, velocity, and acceleration, respectively. Earthquake disturbance force $F(t) = -[M]\{L\}\ddot{x}_g$, where L is an $(n+1)$-dimensional identity matrix; $U(t)$ represents the vector of active inter-storey control forces and D_s, and B_s are the location matrices of the earthquake forces and control forces, respectively.

In state space, Eq. (1) becomes

$$\dot{Z}(t) = AZ(t) + BU(t) + DF(t) \tag{2}$$

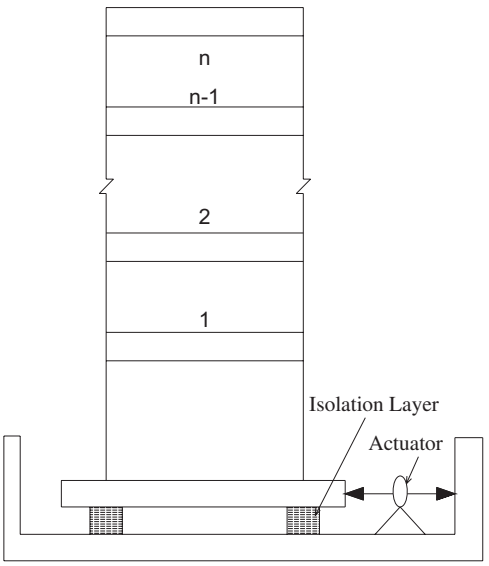

Fig. 1. Model of base-isolation hybrid control system.

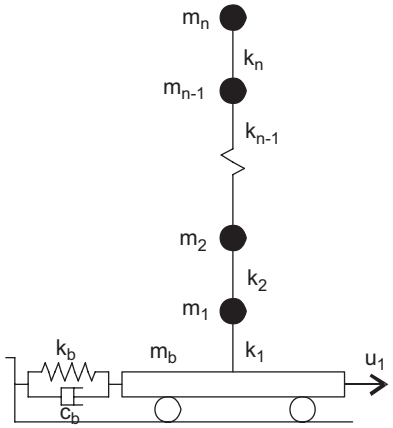

Fig. 2. Analytical model.

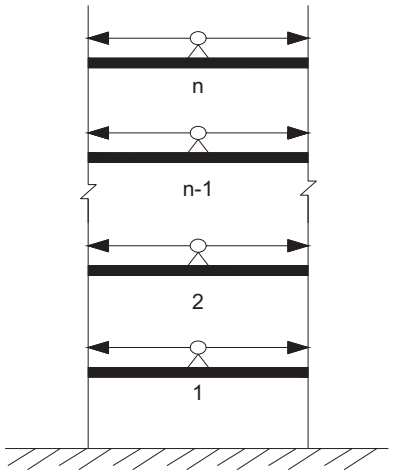

Fig. 3. Structure model of active fixed base control system.

where

$$Z(t)=\begin{bmatrix} Y(t) \\ \dot{Y}(t) \end{bmatrix}, \quad A=\begin{bmatrix} 0 & I \\ -M^{-1}K & -M^{-1}C \end{bmatrix}, \quad B=\begin{bmatrix} 0 \\ M^{-1}B_s \end{bmatrix}, \quad D=\begin{bmatrix} 0 \\ M^{-1}D_s \end{bmatrix}$$

$Z(t)$ is a state vector of order $(2n+2)$; A is a $(2n+2)\times(2n+2)$ system matrix; I is an $(n+1)\times(n+1)$ identity matrix; B and D are matrices of order $(2n+2)\times 1$.

1.2. Active control system of a fixed base frame

The structural and analytical models for the active control system of a fixed base frame (no base-isolation) are shown in Figs. 3 and 4, respectively. Provided each floor of the system has an actuator, the equation of motion of the system can be written as

$$[M]\{\ddot{Y}(t)\}+[C]\{\dot{Y}(t)\}+[K]\{Y(t)\}=D_sF(t)+B_sU(t) \tag{3}$$

where $[M]$, $[C]$, and $[K]$ represent $n\times n$ mass, damping, and stiffness matrices of the structure, respectively; $Y(t)$, $\dot{Y}(t)$, and $\ddot{Y}(t)$ are, respectively, the n-dimensional, inter-storey displacement, velocity, and acceleration

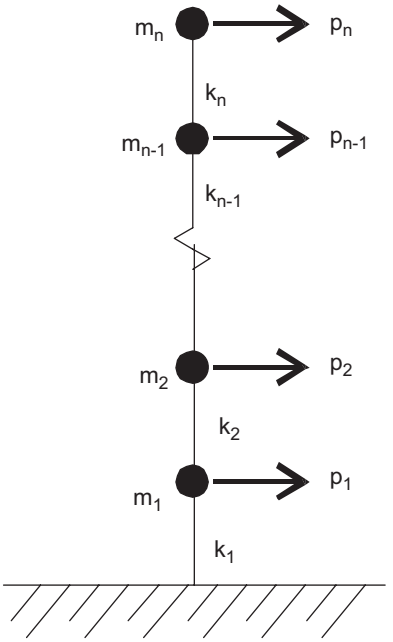

Fig. 4. Analytical model.

vectors of the system; earthquake disturbance force $F(t) = -[M]\{L\}\ddot{x}_g$; where L is an n-dimensional identity matrix; $U(t)$ is the vector of active, inter-storey control forces, and D_s, and B_s are the location matrices of the earthquake forces and control forces, respectively.

In state space, Eq. (3) becomes

$$\dot{Z}(t) = AZ(t) + BU(t) + DF(t) \tag{4}$$

where

$$Z(t) = \begin{bmatrix} Y(t) \\ \dot{Y}(t) \end{bmatrix}, \quad A = \begin{bmatrix} 0 & I \\ -M^{-1}K & -M^{-1}C \end{bmatrix}, \quad B = \begin{bmatrix} 0 \\ M^{-1}B_s \end{bmatrix}, \quad D = \begin{bmatrix} 0 \\ M^{-1}D_s \end{bmatrix}$$

$Z(t)$ is a $2n$ state vector; A is a $2n \times 2n$ system matrix; I is an $n \times n$ identity matrix; B and D are $2n \times n$ matrices.

2. Grey forecasting control

2.1. Principle of grey forecasting model

The working process of a grey forecasting control system is shown in the block diagram of Fig. 5. The output vector Y is measured continuously by a sampling device, after which the values of Y at the time of the kth step are forecast, fed back by the grey forecasting device and compared with target values in terms of system time-delay. The CS is then ascertained, with the objective of making the future output Y close to target value J. Finally, the actuator accepts the CS and applies the control force to the building. The whole control system includes four subsystems: the sampling system, the forecasting system, the control system, and the mechanical force system.

2.2. Grey theory forecasting model

When applying forecasting control, forecasting is obviously the key process within the control system. In this paper, grey forecasting is represented by the block diagram shown in Fig. 6.

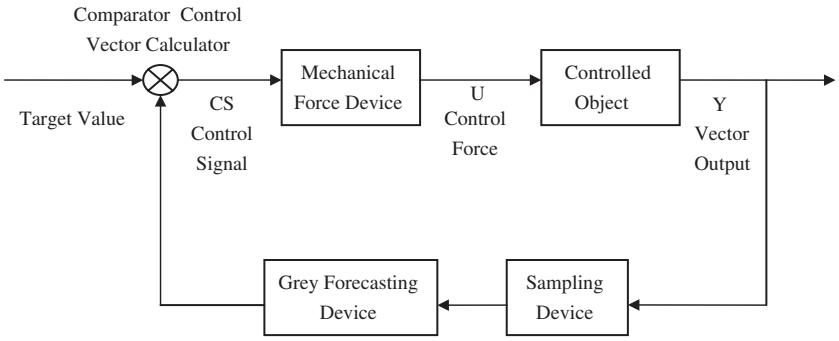

Fig. 5. Block diagram of grey forecasting control principle.

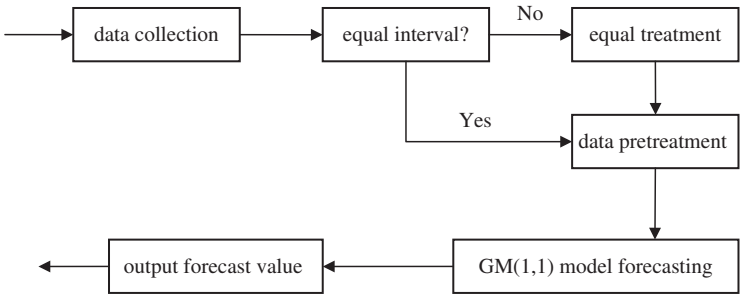

Fig. 6. Block diagram of grey forecasting module.

The process starts with the collection of original data by the data collecting module. After any required equal interval treatment and the pretreatment of the data series, the input demands of the GM(1,1) model are satisfied and the forecast values of the next step may be obtained from the forecast model.

Considering $Z(t)$ as the state vector sample of the system at the present time, and $Z(t-3)$, $Z(t-2)$ and $Z(t-1)$ as samples at earlier times, the raw series can be written as

$$Z^{(0)}(k) = Z(t+k-4) \quad (k = 1, 2, 3, 4) \tag{5}$$

Abbreviating the accumulating generation operation, to AGO, which implies obtaining the generating series through successively adding raw data in series, the AGO series of $Z^{(0)}$ may be written as

$$Z^{(1)}(k) = AGO \cdot Z^{(0)} = \sum_{i=1}^{k} Z^{(0)}(i) \quad (k = 1, 2, 3, 4) \tag{6}$$

The neighbouring mean value series $w^{(1)}$ satisfies

$$w^{(1)}(k) = \tfrac{1}{2}[Z^{(1)}(k) + Z^{(1)}(k-1)] \quad (k = 2, 3, 4) \tag{7}$$

From the generating series $z^{(1)}(k)$, a white differential equation may be obtained as

$$\frac{\mathrm{d}Z^{(1)}}{\mathrm{d}t} + A_g Z^{(1)} = B_g \tag{8}$$

where A_g is the developing coefficient and B_g, the grey input.

The distinguishing parameter vectors $\hat{a} = [A_g, B_g]^{\mathrm{T}}$ may be obtained by the least squares method

$$\hat{a} = \begin{bmatrix} A_g \\ B_g \end{bmatrix} = (V^{\mathrm{T}} V)^{-1} V^{\mathrm{T}} Y_n \tag{9}$$

where V is a $6n \times 4n$-dimensional matrix and Y_n is a $6n$-dimensional vector. V, Y_n can be assembled as

$$V = \begin{bmatrix} w^{(1)}(2,1) & 1 & & & & & & & & & & 0 \\ w^{(1)}(3,1) & 1 & & & & & & & & & & \\ w^{(1)}(4,1) & 1 & & & & & & & & & & \\ & & w^{(1)}(2,2) & 1 & & & & & & & & \\ & & w^{(1)}(3,2) & 1 & & & & & & & & \\ & & w^{(1)}(4,2) & 1 & & & & & & & & \\ & & & & \ddots & & & & & & & \\ & & & & & \ddots & & & & & & \\ & & & & & & & & w^{(1)}(2,n) & 1 & & \\ & & & & & & & & w^{(1)}(3,n) & 1 & & \\ 0 & & & & & & & & w^{(1)}(4,n) & 1 & & \end{bmatrix} \quad Y_n = \begin{bmatrix} Z^{(0)}(2,1) \\ Z^{(0)}(3,1) \\ Z^{(0)}(4,1) \\ Z^{(0)}(2,2) \\ Z^{(0)}(3,2) \\ Z^{(0)}(4,2) \\ \vdots \\ \vdots \\ Z^{(0)}(2,n) \\ Z^{(0)}(3,n) \\ Z^{(0)}(4,n) \end{bmatrix}$$

The solution of the white differential equation can be expressed as

$$\dot{Z}^{(1)}(k+1) = (Z^{(0)}(1) - B_g \cdot / A_g) e^{-A_g k} + B_g \cdot / A_g \tag{10}$$

Applying an inverse accumulating generation operation (IAGO) to $\dot{Z}^{(1)}(k)$, the forecast value of the next step can be obtained as

$$\dot{Z}^{(0)}(k+1) = IAGO \cdot \dot{Z}^{(1)}(k+1) - \dot{Z}^{(1)}(k) \tag{11}$$

After the forecast data has been retrieved and modified to diminish residual error, the final forecast value is obtained as

$$Z^{(0)}(k+1) = -A_g \cdot (Z^{(0)}(1) - B_g \cdot / A_g) \cdot \mathrm{e}^{-A_g k} \pm A_\varepsilon \cdot (\varepsilon^{(0)}(k_0) - B_\varepsilon \cdot / A_\varepsilon) \cdot \mathrm{e}^{-A_\varepsilon (k-k_0)} \tag{12}$$

where $\varepsilon^{(0)}(k) = Z^{(0)}(k) - \dot{Z}^{(0)}(k)$, the calculation methods for A_ε, B_ε are the same as for A_g, B_g, and k_0 is the number of raw data series.

The grey forecasting algorithm is based on the metabolizing model, where the input Z^0 is constantly updated by replacing old data by the newest data, thus ensuring good adaptability of the model.

2.3. Control algorithm

Using the state Eqs. (2) and (4), and applying linear quadratic optimal control theory, the second-order performance index function of the system is defined as [11–13]

$$J = \frac{1}{2} \int_{t_0}^{\infty} [Z^{\mathrm{T}} Q Z + U^{\mathrm{T}} R U] \, \mathrm{d}t \tag{13}$$

where

$$Q = \alpha \begin{bmatrix} K & 0 \\ 0 & M \end{bmatrix}$$

and $R = \beta I$.

Q is the weighted structure state response matrix and R, the weighted matrix of control force vector; α and β are the indefinite coefficients, the values of which may be consulted in Ref. [8]. Considering the extreme condition $\partial J / \partial U = 0$, the optimal control force of system may be expressed as

$$U = -GZ \tag{14}$$

where G is the optimal state feedback gain matrix:

$$G = R^{\mathrm{T}} B^{\mathrm{T}} P(t) \tag{15}$$

and P is the solution to the Riccati algebraic equations, given by

$$-PA - A^{\mathrm{T}} P + PBR^{-1} B^{\mathrm{T}} P - Q = 0 \tag{16}$$

3. Analysis of the control scheme

Consider now a grey forecasting model of a dynamic, closed-loop control system (Fig. 7). The working process in the case of earthquake excitation is as follows. In general, as seismic ground motion is initiated, the magnitude of the response is usually small, but sufficient to cause the sampling devices to start operating. A series of structural response data values (e.g. $Z^{(0)}(k_t)$, where $Z^{(0)}(k_t)$ can represent displacements, velocities accelerations or control forces) are measured and transmitted to the grey forecasting device for determining the forecast value $Z_p(k_{t+m,\Delta t})$ (m represents the forecasting step, $m = t'/\Delta t'$; t', Δt represent the time-delay of the system and the sampling interval, respectively, t is the final time). $Z_p(k_{t+m,\Delta t})$ is transmitted to the comparator and compared with the target value. The control vector U is determined based on Eq. (12) and the target value and then output to the actuators. Based on U, the actuators apply the control forces to the structure. The next state vectors $\mathbf{Z}(k+1)$ for modeling will be generated, measured by the sampling device as new data and input into the next forecasting control cycle. The cycles continue until the ground excitation or response falls below a predetermined threshold and the control process ends.

4. Example 1

Consider a five-storey, reinforced concrete frame structure with base-isolation, subjected to an earthquake ground motion. The structural model and analytical model are shown in Figs. 1 and 2. The lumped mass and shear stiffness of the building are 3×10^5 kg and 2×10^8 N/m per storey. The mass and stiffness of the isolation layer are 2.4×10^5 kg and 2×10^8 N/m, respectively. Assuming that the damping ratio of the superstructure is $\xi = 0.05$, and the damping ratio of isolation layer is 0.10, the control parameters have the values $\alpha = 100$ and

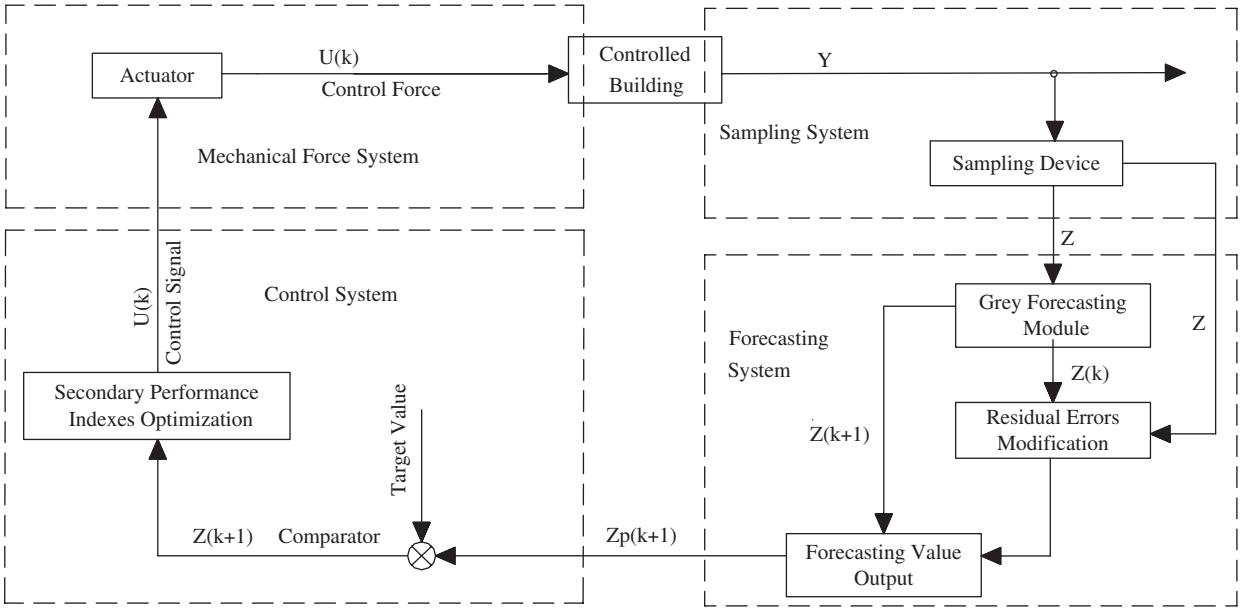

Fig. 7. Flow diagram of grey forecasting control system.

$\beta = 1 \times 10^{-5}$. Excitation is from the El-Centro (NS, 1940) earthquake ground motion record, with a peak acceleration of 200 gal, and a sampling interval of 0.02 s. Time-delay of the system is taken as 0.02 s, which equates to one sampling interval. Based on the parameters above, the time–history response of the structure was calculated using a Matlab programme [14]. Five cases were analysed:

① Without any vibration-reducing technique.
② Base-isolation only.
③ Base-isolation and active control at isolation layer with a zero time-delay.
④ Control technique as in case 3 but a time-delay of 0.02 s. Influence of time-delay on structural control is analysed.
⑤ Control technique as in case 3 but with consideration of the 0.02 s time-delay. Grey forecasting control model employed.

The resulting structural responses and control forces are shown in Tables 1–4 and Figs. 8–14.

4.1. Analysis of control effect

Table 1 , Figs. 8 and 10 show that both cases 2 and 5 reduce displacement of the superstructure by about 85 percent compared with the fixed base (un-isolated) case 1. Displacement of the base-isolation layer in the uncontrolled case 2 is about 20 times that of the superstructure. Active control of the isolation layer, reduces this displacement to about 50 percent of its uncontrolled value as shown in Figs. 9 and 11, moving the deformation of the isolation layer into a safer and more manageable range. Table 3 and Fig. 9 show that the combination of base-isolation and hybrid control can effectively reduce the acceleration of the structure at all levels, particularly that of the top floor, where acceleration is reduced to about half that of the uncontrolled case. The variation with height of the displacement and acceleration responses for the three cases 1, 2, and 5 vary as shown in Figs. 11 and 12. The acceleration of the structure without control starts at a higher value and increases rapidly with height. The acceleration of each floor of the structure with the actively controlled isolation layer (case 5) exceeds that of the uncontrolled case 2 by a small amount, diminished with height.

Table 1
Maximum displacement of the model structure (cm).

Condition	①	②	③	④	⑤
Floor					
0		7.59	3.68	3.67	3.67
1	2.27	0.34	0.38	0.43	0.37
2	2.05	0.31	0.35	0.38	0.37
3	1.68	0.25	0.27	0.27	0.26
4	1.22	0.18	0.18	0.18	0.18
5	0.67	0.09	0.08	0.1	0.08

Table 2
Maximum velocity of the model structure (m/s).

Condition	①	②	③	④	⑤
Floor					
0		0.295	0.14	0.14	0.145
1	0.173	0.304	0.143	0.145	0.144
2	0.321	0.307	0.171	0.176	0.173
3	0.437	0.308	0.205	0.213	0.208
4	0.514	0.308	0.233	0.240	0.236
5	0.56	0.307	0.254	0.264	0.259

Table 3
Maximum acceleration of the model structure(m/s^2).

Condition	①	②	③	④	⑤
Floor					
0		1.83	2.504	2.635	2.655
1	3.232	1.814	2.421	2.357	2.294
2	3.863	1.884	2.423	2.471	2.591
3	4.064	2.003	2.26	2.378	2.282
4	4.433	2.083	2.341	2.515	2.472
5	4.765	2.114	2.434	2.467	2.452

Table 4
Maximum control force (kN).

Condition	③	④	⑤
Floor			
0	611	619	651

Floor 0 is isolation layer, condition 1 has no isolation layer.

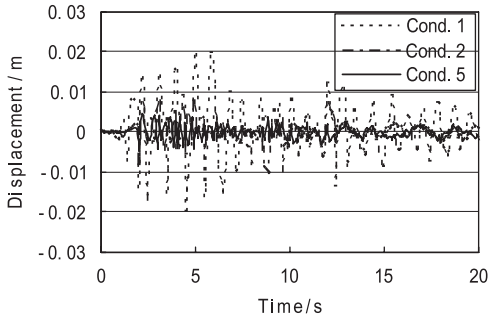

Fig. 8. Displacement response of first floor.

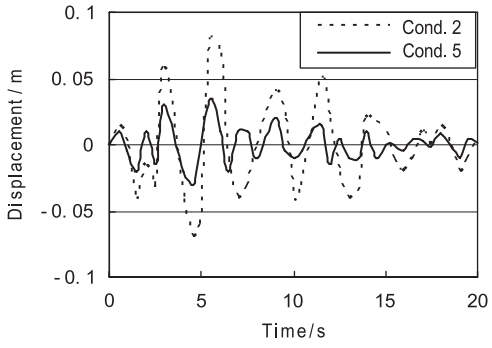

Fig. 9. Displacement response of isolation layer.

4.2. Analysis of precision

Regarding the control force and the structure responses, both the forecasting control and the time-delay control deviate from the ideal state of immediate control. If the time-delay is very small, the deviations can be

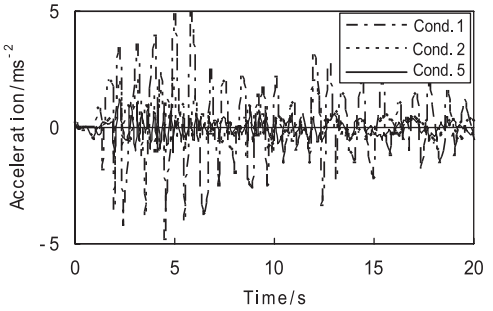

Fig. 10. Acceleration response of the top floor.

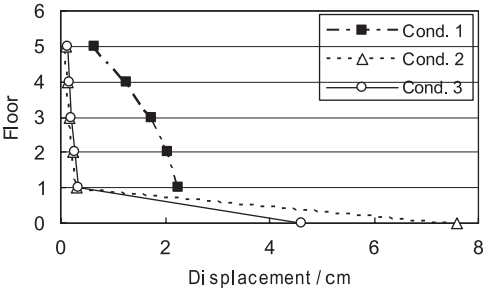

Fig. 11. Maximum displacement response of each floor for cases ①, ②, and ⑤.

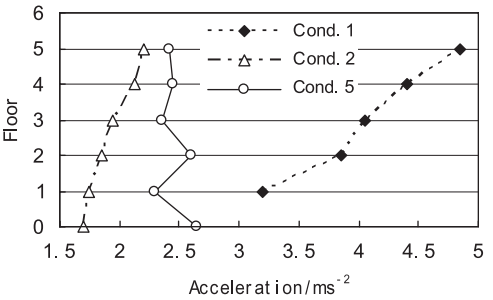

Fig. 12. Maximum acceleration response of each floor under cases ①, ②, and ⑤.

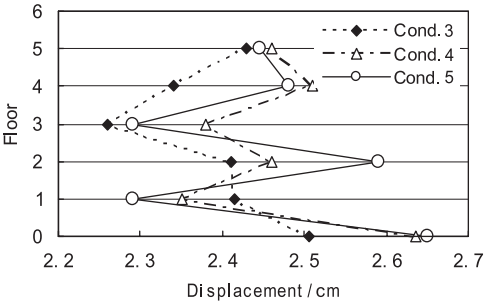

Fig. 13. Maximum acceleration response of each floor cases ③–⑤.

neglected, but the error-generating principles are different. In the former control method, the deviation is determined by the forecasting error, which makes the response diverge from the ideal state. In the latter control method, the deviation is caused by the time-delay, which magnifies the structure response. The degree

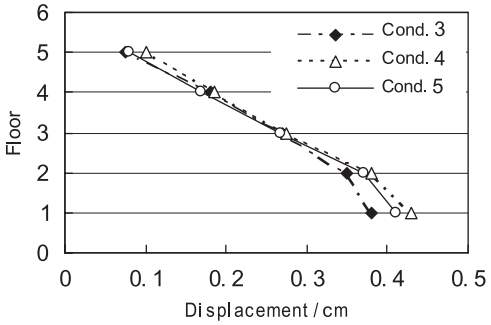

Fig. 14. Maximum displacement response of each floor cases ③–⑤.

of magnification is determined by the magnitude of the time-delay. If the time-delay is very big, it will lead to divergent response. Thus, the curve of case 5 approaches that of case 3, while the curve of case 4 trends to deviate from that of case 3.

5. Optimal GM(1,1) grey forecasting model

The background value is one of the key factors influencing the control process. Based on the exponential function form of the model, the background value may be determined by an integral formula, allowing the original background value to be optimized. Hence a modified grey forecasting model based on the optimal background value can improve the forecast precision and overcome the delay errors arising in the original grey forecasting model.

5.1. Optimization of background value

From Eq. (12), the simulation and prediction precision of the GM(1,1) model depend on parameters A_g and B_g, which in turn rely on the raw data series and form of the background value, $w^{(1)}(k)$. $w^{(1)}(k)$ is one of the key factors influencing the simulation error $\varepsilon^{(0)}(k) = \hat{z}^{(1)}(k) - z^{(1)}(k)$ and the applicability of the GM(1,1) model.

Thus Eq. (8) may be integrated from k to $k+1$(Fig. 15),

$$Z^{(1)}(k+1) - Z^{(1)}(k) + A_g \int_k^{k+1} Z^{(1)}(t)\,\mathrm{d}t = B_g \quad k = 1, 2, \ldots, n-1 \tag{17}$$

Assuming $w^{(1)}(K+1)$ is the background value of $z^{(1)}(t)$ in the interval $[k, k+1]$, there results [10]

$$\int_k^{k+1} z^{(1)}(t)\,\mathrm{d}t = [(k+1) - k]w^{(1)}(k+1) = w^{(1)}(k+1) \tag{18}$$

Eq. (18) shows that the background value is the definite integral of $z^{(1)}(t)$ in the interval $[k, k+1]$. Because the solution of Eq. (8) is in an exponential format, $z^{(1)}(t)$ can be written as

$$z^{(1)}(t) = c\mathrm{e}^{bt} \tag{19}$$

with the curve passing through the points $z^{(1)}(k)$ and $z^{(1)}(k+1)$, thus

$$z^{(1)}(k) = c\mathrm{e}^{bk} \tag{20}$$

$$z^{(1)}(k+1) = c\mathrm{e}^{b(k+1)} = c\mathrm{e}^{bk} \cdot \mathrm{e}^{b} \tag{21}$$

From (20) and (21) we have

$$b = \ln\left[\frac{z^{(1)}(k+1)}{z^{(1)}(k)}\right] = \ln z^{(1)}(k+1) - \ln z^{(1)}(k) \tag{22}$$

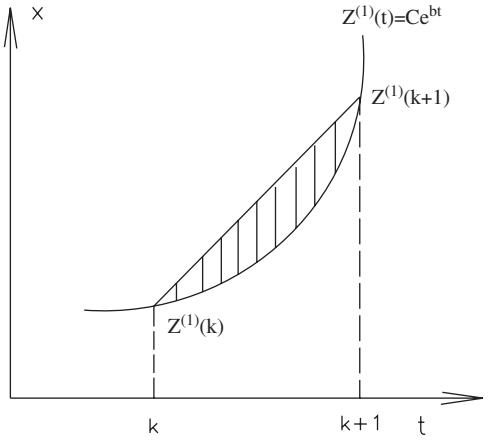

Fig. 15. A schematic diagram showing reasons for error from original model GM(1,1).

$$c = \frac{z^{(1)}(k)}{e^{bk}} = \frac{z^{(1)}(k)^{k+1}}{z^{(1)}(k+1)^{k}} \tag{23}$$

Thus optimal background value is [15,16]

$$w^{(1)}(k+1) = \int_{k}^{k+1} z^{(1)}(t)\,dt = \int_{k}^{k+1} ce^{bt}\,dt = \frac{c}{b}(e^{b(k+1)} - e^{bk}) = \frac{z^{(1)}(k+1) - z^{(1)}(k)}{\ln z^{(1)}(k+1) - \ln z^{(1)}(k)} \tag{24}$$

Let

$$y_n = [z^{(0)}(2), z^{(0)}(3), z^{(0)}(4), \ldots, z^{(0)}(n)]^{\mathrm{T}} \tag{25}$$

$$B = \begin{pmatrix} -w^{(1)}(2) & 1 \\ -w^{(1)}(3) & 1 \\ \cdots & \cdots \\ -w^{(1)}(n) & 1 \end{pmatrix} \tag{26}$$

5.2. Parameters a and u for establishing the optimal GM(1,1) model

The parameter vectors $\hat{a} = [A_g, B_g]^{\mathrm{T}}$ may be obtained by the least squares method

$$\hat{a} = [B^{\mathrm{T}}B]^{-1}B^{\mathrm{T}}y_n \tag{27}$$

Substituting Eq. (27) into Eq. (8), and letting $x^{(1)}(t)_{t=1} = x^{(0)}(1)$, there results

$$\hat{Z}^{(1)}(t) = \left[Z^{(0)}(1) - \frac{B_g}{A_g}\right]e^{-A_g(t-1)} + \frac{B_g}{A_g} \tag{28}$$

For AGO series $X^{(1)}(k)$, we have

$$\hat{Z}^{(1)}(k+1) = \left[Z^{(0)}(1) - \frac{B_g}{A_g}\right]e^{-A_g k} + \frac{B_g}{A_g} \tag{29}$$

In Eq. (29), $\hat{Z}^{(1)}(k)$ is determined by means of an IAGO, allowing the predicted value of $Z^{(0)}(k)$ to be expressed as

$$\begin{cases} \hat{Z}^{(0)}(1) = Z^{(0)}(1) \\ \hat{Z}^{(0)}(k+1) = \hat{Z}^{(1)}(k+1) - \hat{Z}^{(1)}(k) = (1 - e^{A_g})\left[Z^{(0)}(1) - \frac{B_g}{A_g}\right] e^{-A_g k} \end{cases} \tag{30}$$

6. Example 2

Consider a five-storey reinforced concrete frame structure subjected to earthquake ground motion based on the El-Centro (NS, 1940) record with a peak acceleration of 200 gal. The parameters are as follows: the lumped mass and shear stiffness of the building are 4.5×10^5 kg and 3×10^8 N/m per storey; the damping ratio $\zeta = 0.05$, the control parameters $\alpha = 150$ and $\beta = 1 \times 10^{-5}$. We consider a time-delay of 0.02 s for the earthquake wave with a sampling interval of 0.04 s or a time-delay of 0.06 s for the earthquake wave with a sampling interval of 0.02 s. Five cases were analysed using the time-history analysis programme implemented in Matlab: ① no control, ② control without forecasting, ③ grey forecasting control based on GM(1,1) model, and ④ grey forecasting control based on the optimal GM(1,1) model. The resulting structural responses and control forces are shown in Table 5 and Figs. 16–21.

6.1. Analysis of grey forecasting control effect

Table 5 and Fig. 16 show that compared with case 1, the inter-storey displacements of the superstructure are reduced in cases 2–4, where the sampling interval of the earthquake wave is 0.04 s and the time-delay is 0.02 s. The control effect on the bottom floor is especially obvious, which has a 50 percent reduction. Fig. 17 shows the control effect on acceleration of the top floor where there are 30 percent reductions in cases 2–4. The control technique clearly improves the safety and comfort of occupants during the earthquake. For the earthquake wave with a sampling interval of 0.02 s and time-delay of 0.06 s, the results in Table 5 and Fig. 18 also show a good reduction in the inter-storey displacement in cases 2–4. Due to the influence of time-delay, the magnitude of the reduction is decreased, especially in case 2. The maximum acceleration of the top floor without forecasting control is reduced by about 16 percent, compared with a 35 percent reduction under forecasting control (Fig. 19), showing that forecasting control not only overcomes the influence of time-delay, but also reduces the disturbance error because of differences of sampling intervals.

Table 5
Maximum response and controlling force of structure as a result of earthquake action.

Item	Maximum displacement (cm)			Maximum acceleration (m/s^2)			Maximum control force (kN)		
Condition	First floor	Third floor	Fifth floor	First floor	Third floor	Fifth floor	First floor	Third floor	Fifth floor
(a) *sampling interval* 0.04 *s and time-delay* 0.02 *s*									
①	2.27	1.69	0.68	2.122	3.464	4.522			
②	1.22	1.03	0.47	1.785	2.104	3.122	1080	867	322
③	1.22	0.97	0.45	1.84	2.091	3.006	1160	911	341
④	1.22	0.97	0.45	1.836	2.089	3.001	1162	912	341
(b) *Sampling interval* 0.02 *s and time-delay* 0.06 *s*									
①	2.27	1.69	0.68	2.122	3.463	4.521			
②	1.39	1.16	0.58	2.379	2.676	3.783	1191	948	325
③	1.25	0.98	0.46	2.063	2.663	2.956	1448	1107	404
④	1.25	0.98	0.46	2.056	2.669	2.949	1448	1106	403

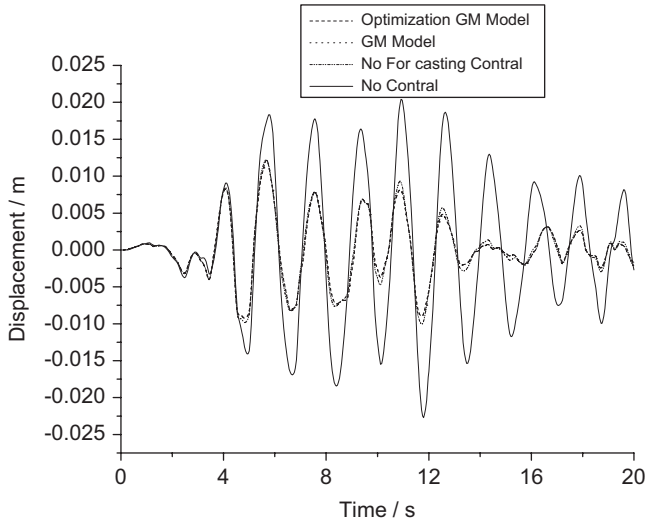

Fig. 16. Relative deformation of first floor with sampling period of 0.04 s.

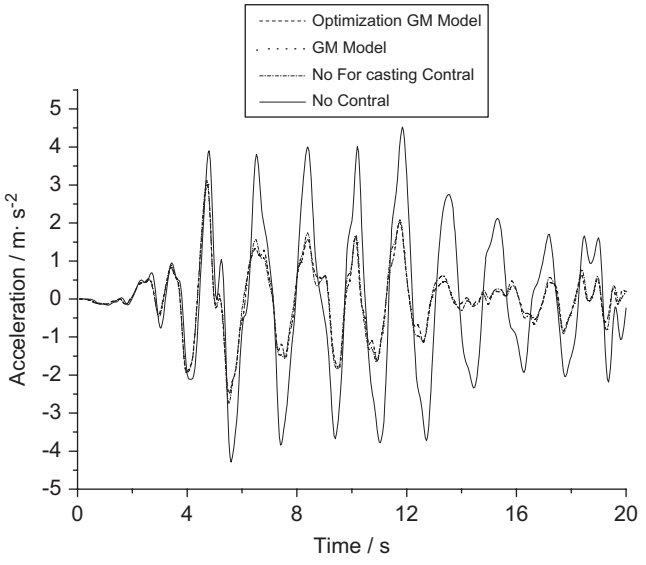

Fig. 17. Absolute acceleration of top floor as sampling period is 0.04 s.

6.2. Comparison of the control precision

The prediction precision of the optimal and non-optimal GM(1,1) models are compared in terms of the difference value which represents the difference between the forecasting control displacement and immediate control displacement. Fig. 20 shows that for an earthquake wave with the sampling interval of 0.04 s, the prediction precision of optimal GM(1,1) model is superior to GM(1,1) model in terms of the error value of displacement of the bottom floor. For the case with sampling interval of 0.02 s and time-delay of 0.06 s, the maximum acceleration error value of optimal GM(1,1) are a little lower than that of GM(1,1) as shown in Fig. 21. The reason is the increased time-delay and forecasting step. As regards the difference in value of the acceleration on the top floor, the optimal GM(1,1) model shows a higher precision than the GM(1,1) model.

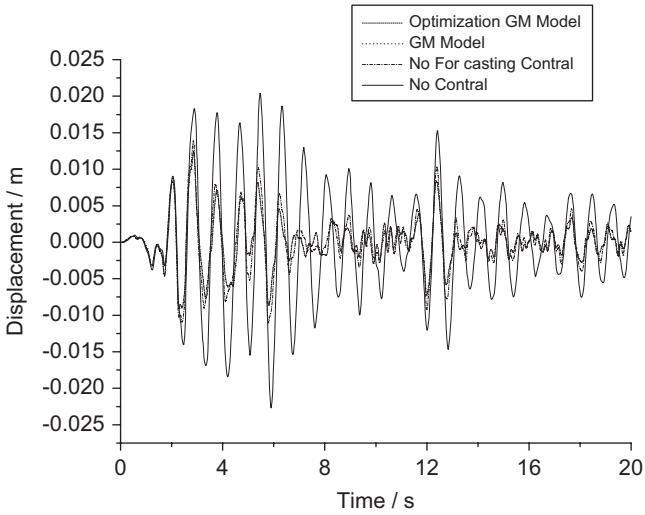

Fig. 18. Relative deformation of first floor with sampling period of 0.02 s.

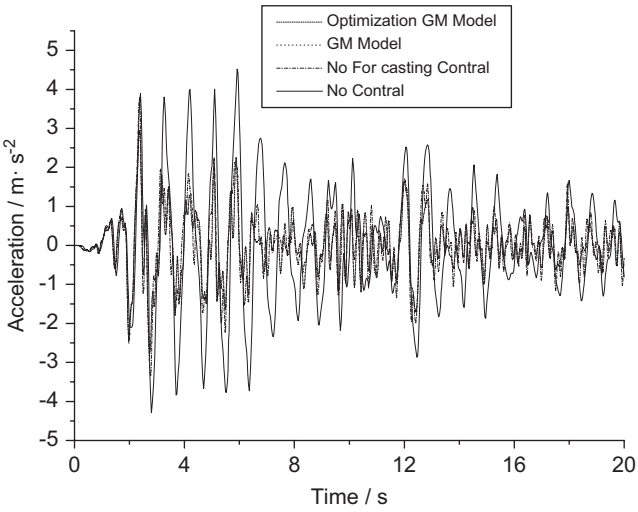

Fig. 19. Absolute acceleration of top floor with sampling period of 0.02 s.

7. Conclusions

The grey forecasting control model can overcome the lagging control error caused by time-delay and the original data disturbance error caused by a different sampling interval for earthquake data. There is also no need to establish a structural model or to consider the change of structure parameters (e.g. stiffness and damping) because the grey forecasting GM(1,1) control process obtains all the necessary information by sampling the structure's response. Therefore, the grey forecasting control based on the GM(1,1) model and the optimal GM(1,1) model is simple, effective, and reliable. Numerical results also show its higher prediction precision and better control effect compared with the GM(1,1) model. Therefore, the grey forecasting control technique based on the optimal GM(1,1) model is more effective and practical than the original one in the structure vibration control field.

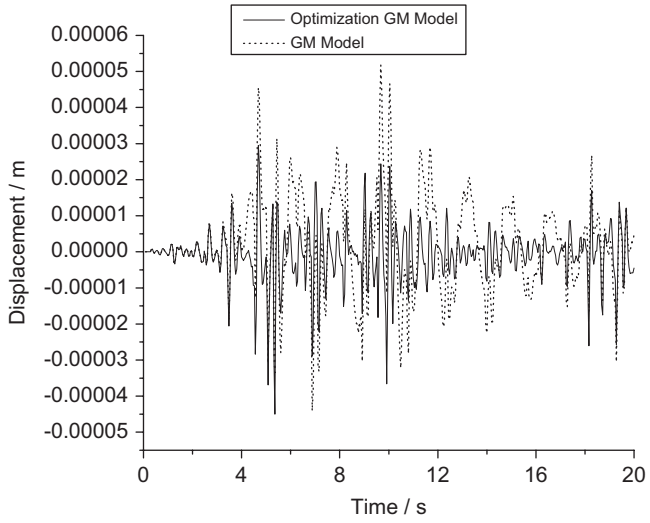

Fig. 20. Deformation error of first floor with sampling period of 0.04 s.

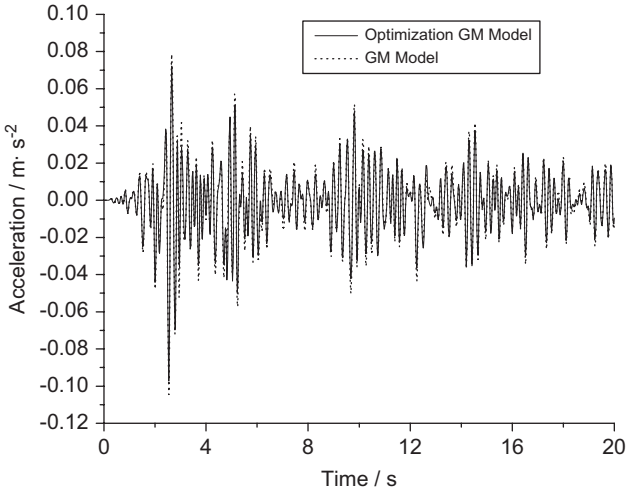

Fig. 21. Absolute acceleration error of top floor with sampling period of 0.02 s.

Acknowledgements

The writers are grateful for the financial support from the Lanzhou Jiaotong University through its "qinglan rencai" Development Programme in Structural Vibration Control.

References

[1] G.W. Housner, L.A. Bergman, T.K. Caughey, A.G. Chassiakos, et al., Structural control of past, present and future, *Journal of Engineering Mechanics—ASCE* 123 (9) (1997) 897–971.
[2] B.F. Spencer Jr., M.K. Sain, Controlling buildings: a new frontier in feedback, *IEEE Control System Magazine* 17 (6) (1997) 19–35.
[3] Y.F. Du, Sequential optimal control algorithm for hysteretic smart isolated structures, *Chinese Journal of Computational Mechanics* 24 (1) (2007) 57–62.
[4] A.K. Agrawal, J.N. Yang, Compensation of time-delay for control of civil engineering structures, *Earthquake Engineering & Structural Dynamics* 29 (1) (2000) 37–41.

[5] Z.X. Wang, C.D. Wu, The establishment and application of a improved GM(1,1) model, *Mathematics in Practice and Theory* 33 (9) (2003) 20–25.
[6] B. Zhao, X.L. Lu, M.Z. Wu, et al., Sliding mode control of buildings with base-isolation hybrid protective system, *Earthquake Engineering & Structural Dynamics* 29 (3) (2000) 315–323.
[7] L.L. Chung, C.C. Lin, K.H. Lu, Time-delay control of structure, *Earthquake Engineering & Structural Dynamics* 24 (3) (2003) 687–701.
[8] T.T. Soong, *Active Structural Control Theory and Practice*, Longman, New York, USA, 1990.
[9] S.F. Liu, J.L. Deng, The range suitable for GM(1,1), *Systems Engineering Theory & Practice* 5 (5) (2000) 121–124.
[10] C.X. Li, C.F. Han, Discussion on time-delay compensation of active control of building structures under earthquakes, *Journal of Xi'an University of Architecture & Technology* 30 (2) (1998) 138–140.
[11] D. Luo, S.F. Liu, Y.G. Dang, The optimization of grey model GM(1,1), *Engineering Science* 8 (2003) 50–53.
[12] L.H. Zou, *Study of Some Problems on Vibration-Reduction Control of Engineering Structure[D]*, Southwest Jiaotong University, 2004.
[13] J.Y. Du, X.M. Wang, et al., Study and implementation of the algorithms for active environment noise control, *Noise and Vibration Control* 2 (1) (2007) 93–96.
[14] S.H. Zhang, S.J. Liu, et al., Research of CBR, DM and smart algorithms based design methods for high-rise building structure form-selection, *Journal of Harbin Institute of Technology* 13 (3) (2006) 325–332.
[15] W. Zeng, Y.P. Liu, et al., Simulation of active vibration control system on MATLAB/simulink, *Journal of Beijing University of Technology* 32 (6) (2006) 102–106.
[16] G.H. Bi, L.H. Zou, C. Wang, Study of optimal control for the vibration of a building structure based on the grey forecasting to seismic wave, *Journal of Lanzhou Jiaotong University (Natural Sciences)* 25 (1) (2006) 14–16.